J. Fluid Mech. (1967), *vol.* 30, *part* 2, *pp.* 259–284
Printed in Great Britain

On the light-scatter technique for the study of turbulence and mixing

By H. A. BECKER

Department of Chemical Engineering, Queen's University at Kingston, Ontario, Canada

H. C. HOTTEL AND G. C. WILLIAMS

Department of Chemical Engineering, Massachusetts Institute of Technology

(Received 6 September 1966 and in revised form 4 July 1967)

The light-scatter technique facilitates study of the concentration field when one of the streams entering a mixing region is marked with colloidal particles. The present paper provides basic information for the effective application of the technique. The system response is analysed theoretically. The problems of noise and spatial resolution are examined and experimental data are presented from which the response parameters are evaluated numerically. The capabilities of the technique for characterizing turbulent concentration fluctuations are described. The technique is excellent in the convection region of the turbulence spectrum but fails where molecular diffusion is important.

1. Introduction

The light-scattering property of colloidal dispersions can be utilized for the detection of concentration fluctuations accompanying turbulent mixing. In the initial study Rosensweig, Hottel & Williams (1961) investigated isothermal air–air free jet mixing in which the nozzle fluid was an oil/air smoke. Subsequent work has dealt with free and confined jet mixing (Becker, Hottel & Williams 1963, 1965, 1967; Williams & Becker 1963), turbulent dispersion in a pipe flow (Becker, Rosensweig & Gwozdz 1966), mixing in the well-stirred reactor (Hottel, Williams & Miles 1967), and temperature-induced concentration fluctuations in a turbulent flame (Gurnitz 1966). Since the technique provides a powerful tool for investigating turbulence and mixing, the present paper presents the theory and measurements essential to indicate its capabilities and limitations.

The principle of the technique is illustrated in figure 1. One of the streams entering a mixing field is marked with a sol (in gases, a smoke or fog). Light scattered by the sol from a beam projected into the field is intercepted by an optical system at one side and focused on a slitted diaphragm. The slit passes to a phototube the light scattered from a short segment of the incident beam. The electrical signal thereby produced is ideally proportional to the amount of sol in the defined control volume, and, when that volume is small enough, to the point concentration. The response of the phototube is linear in light flux in the normal range of loading and up to *ca.* 10^8 c/s. Thus the problems of non-linearity which

complicate most methods of turbulence study are absent. However, the technique has other difficulties and limitations, the description and analysis of which follows.

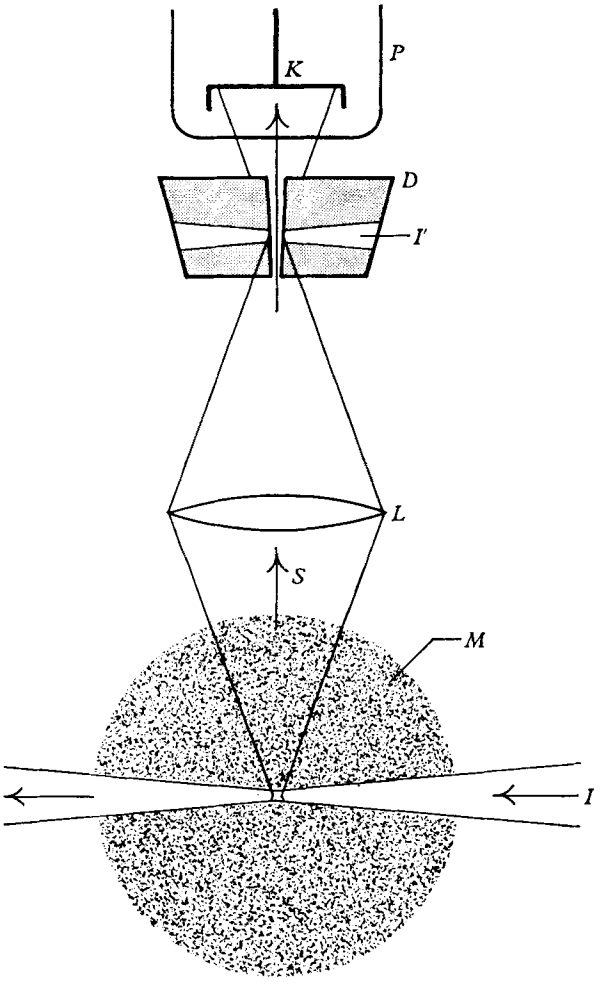

FIGURE 1. The principle of the light-scatter technique. M, mixing field; I, incident beam; S, scattered-light beam; D, slitted diaphragm; L, lens system; I', scattered-light image of incident beam on diaphragm; P, multiplier phototube; K, photocathode.

2. The phototube response

The phototube response to scattered light

When light of spectral intensity J_i irradiates a spherical particle through a solid angle $d\omega_i$, the energy flux scattered into a solid angle $d\omega_s$ in a direction at angle θ to the incident beam is

$$\tfrac{1}{4}\pi D_p^2 d\omega_i d\omega_s \int_0^\infty \psi(\pi D_p/\lambda, \theta, n_p)\, J_i d\lambda, \tag{1}$$

where D_p and n_p are the particle diameter and index of refraction, and $\frac{1}{4}\pi D_p^2 J_i d\lambda d\omega_i$ is the flux incident on the particle in a wavelength interval $d\lambda$.

For wavelengths large relative to the particle perimeter, $\lambda > 10\pi D_p$, the scatter function ψ is given by Rayleigh's law:

$$\psi = \frac{1}{2\pi}\left[\frac{\pi D_p}{\lambda}\right]^4\left[\frac{n_p^2-1}{n_p^2+1}\right]^2[1+\cos^2\theta]. \tag{2}$$

When the wavelength is small, ψ tends to be independent of D_p and λ. In general ψ is given by Mie's equations (see the book by Van de Hulst (1957) and numerical solutions by Gucker & Cohn (1953) and Erickson (1961)).

Under normal conditions for the light scatter technique, the flux scattered from a small fixed spatial region or control volume V by the N like particles which are momentarily inside it is N times that scattered by one particle. The spectral intensity of the incident light approximates

$$J_i = J_0\tau_L\tau_1\tau_i,$$

where J_0 is the source intensity (the radiant flux leaving the lamp arc or filament in the direction of projection per unit of arc or filament surface per steradian), and τ_L, τ_1 and τ_i are the spectral transmissivities of the lamp window, the projection optics, and the interposed region of the mixing field. The energy flux incident on the phototube cathode is then

$$\int_0^\infty \Phi_K d\lambda = \tfrac{1}{4}\pi D_p^2 N\omega_i\omega_s\int_0^\infty \psi_{\mathrm{av}}\tau_L\tau_1\tau_i\tau_s\tau_2\tau_P J_0 d\lambda, \tag{3}$$

where τ_s, τ_2 and τ_P are the spectral transmissivities of the mixing field along the scattered beam, the viewing optics, and the phototube window; ω_i and ω_s are the solid angles of divergence of the incident and scattered beams; and ψ_{av} is the average of ψ over ω_i and ω_s. The resulting anode current response of the phototube is

$$I = A\int_0^\infty s_K\,\Phi_K d\lambda \equiv \int_0^\infty s\Phi_P d\lambda, \tag{4}$$

where s_K is the spectral sensitivity of the photocathode, A is the over-all gain of the multiplier stages of the phototube, $s \equiv As_K\tau_P$ is the overall radiant sensitivity of the phototube, and $\Phi_P \equiv \Phi_K/\tau_P$ is the cathode-directed spectral energy flux incident on the phototube window. A typical spectral response characteristic (the graph of s *vs.* λ) is usually included in manufacturer's literature on phototubes. Data are also available on most lamps of interest giving the spectrum of the leaving radiation in the normal direction of projection. Thus, when the system characteristic $\tau_1\tau_2$ is known as a function of wavelength, it is possible to compute the magnitude of the output signal from theory. However, the chief practical value of the above equations is to guide the optimization of performance.

The scattered-light technique may be used directly to study the concentration field of the marking material, and indirectly to study the concentration field of the material of the marked stream. In either case the desired information is partly obscured by superimposed noise, the important types of which will now be considered.

Optical attenuation noise

The signal-attentuating effects of absorption and scatter along the optical path through the mixing field are lumped by joining (3) and (4) to give

$$I = \tfrac{1}{4}\pi D_p^2 N \omega_i \omega_s \tau_{\mathrm{mf}} \int_0^\infty s_K \psi_{\mathrm{av}} \tau_L \tau_1 \tau_2 \tau_P J_0 d\lambda, \tag{5}$$

where τ_{mf} is the over-all transmissivity of the mixing field, defined as the ratio between the actual response of the phototube and the response in the absence of intervening absorption and scatter. τ_{mf} generally varies with the position of the object control volume in the mixing field and is moreover modulated by concentration fluctuations along the optical path. Consequently the signal-reducing response component $I(1-\tau_{\mathrm{mf}})/\tau_{\mathrm{mf}}$ is a complex noise which should be minimized to a degree consistent with over-all optimization.

Practically, the condition $1-\tau_{\mathrm{mf}} \ll 1$ is easily tested for by projecting a beam through the mixing field and observing the modulation of the emergent beam by the presence of the marker. In our work to date it has always been possible to operate at low enough marker concentrations so that optical attenuation noise was a negligible factor.

Optical background noise

The possible causes of optical background noise are: (i) light from extraneous sources; (ii) stray light from the exciting lamp, light from the incident beam, and scattered light from the mixing field, all reflected from the surroundings; (iii) rescatter of scattered light in the mixing field; and (iv) emission from the mixing field, as in flames. In laboratory situations it is usually not difficult to block extraneous sources and to adequately blacken the surroundings. Rescatter should not give trouble if the optical attenuation noise is negligible, $1-\tau_{\mathrm{mf}} \ll 1$. Emission by the mixing field can be coped with by using a lamp, usually the mercury arc, which radiates strongly in a different part of the spectrum together with appropriate filters and optical components.

A quantitative accounting is possible if the anode currents I_b and I_s produced by the background radiation and by light scattered from the object control volume are statistically steady. The total mean response is then $\bar{I} = \bar{I}_s + \bar{I}_b$. The mean squares of the fluctuations $i_s \equiv I_s - \bar{I}_s$ and $i_b \equiv I_b - \bar{I}_b$ are directly additive if the fluctuations are uncorrelated; $\overline{i^2} = \overline{i_s^2} + \overline{i_b^2}$ if $\overline{i_s i_b} \ll \overline{i_s^2}$ or $\overline{i_b^2}$, where $i \equiv I - \bar{I}$.

Background radiation can be characterized by studying the phototransducer response (i) with the incident beam off, and (ii) with the incident beam on, but with the control volume screened from view.

Source fluctuation noise

If the object is to characterize concentration fluctuations then it is desirable that the source intensity be a constant. Suppose a significant fixed level of ripple and random fluctuation is however present. The source spectral intensity J_0 is written

$$J_0 = \bar{J}_0 + j_0 \equiv \bar{J}_0(1+\beta), \tag{6}$$

where j_0 is the fluctuating component, to be regarded as noise, and $\beta \equiv j_0/\bar{J}_0$ should be virtually the same for all light wavelengths if the ripple is small. The incorporation of the factor $1+\beta$ into the over-all phototube response will be considered later.

In some applications modulation or chopping of the incident beam may be desirable, e.g. in order to separate the signal from background noise. The treatment of the results is straightforward and will not be considered here.

Dark noise

The phototube current produced by spurious mechanisms, chiefly thermal emission, is normally independent of the light flux on the photocathode and is therefore called the dark current. The resultant noise is usually a negligible factor in the scattered-light technique. If need be, thermal emission can be suppressed by refrigerating the phototube. A mu-metal shield for magnetic screening is helpful.

Marker shot noise

The number of sol particles in the object control volume V, while usually great, may yet not be so large as to completely validate the assumption of a marker continuum. The particulate nature of the marker then comes into evidence through a random fluctuation or 'shot' noise.

Suppose that, at an instant when the number of sol particle sin V is N, the number which would portray continuum or large-population behaviour is $\tilde{N}$. If V is a region in a thoroughly mixed or 'uniformly marked' steady stream, then $\tilde{N}$ is simply $\overline{N}$, the time-mean number of particles in V. In a turbulent mixing field, however, both N and $\tilde{N}$ fluctuate, with $\tilde{N}$ following the turbulent fluctuations and $N-\tilde{N}$ the excursions from continuum behaviour. Suppose a statistically large number of simultaneous determinations of N and $\tilde{N}$ is made, and focus attention on those values of $\tilde{N}$ lying in a small range $d\tilde{N}$. With N following the Poisson distribution, the mean-square ensemble average of $N-\tilde{N}$ is

$$\langle (N-\tilde{N})^2 \rangle = \tilde{N}.$$

The value of $\tilde{N}$ is in the prescribed range for a fraction of time $d\chi$. The time-average of $(N-\tilde{N})^2$ is therefore

$$\overline{(N-\tilde{N})^2} = \int_0^1 \tilde{N}\, d\chi = \overline{N}.$$

Thus the relative mean-square fluctuation level introduced into the system response by the particulate nature of the marker is, as reported by Rosensweig *et al.* (1961),

$$\frac{\overline{(N-\tilde{N})^2}}{\overline{N}^2} = \frac{1}{\overline{N}}. \tag{7}$$

To a first approximation, the variation in N is attributable to the translation of a frozen concentration pattern through the control volume V at the local mean velocity $\overline{U}$. The average time taken by $\overline{N}$ particles to move through V is $\Delta t = \pi D/4\overline{U}$, where D is the diameter of the object segment of the incident light beam. Consequently each instantaneous sampling of the contents of V is roughly equivalent to a measurement of the transport of particles into V over a sampling

time Δt. Further, if each time record of N and $\tilde{N}$ is representable by a Fourier series, a running record of the input into V over periods Δt is equivalent to recording the flux into V as a function of time through a low-pass filter of bandwidth $\Delta f_V = 1/2\Delta t \cong 2\bar{U}/\pi D$ (the factor 2 comes from the fact that the pass band extends mathematically from $0-\Delta f_V$ to $0+\Delta f_V$; see, for example, Bendat (1958)). For the noise in a band from f to $f+\Delta f$, with $f+\Delta f < \Delta f_V$, we can thus write, from (7),

$$\frac{\overline{(N-\tilde{N})^2}|_{f,\Delta f}}{\bar{N}^2\Delta f} = \frac{\overline{(N-\tilde{N})^2}}{\bar{N}^2\Delta f_V} = \frac{\pi D}{2(\bar{N}/V)V\bar{U}}. \tag{8}$$

This shows how the relative spectral density function of $N-\tilde{N}$ varies with operating conditions.

Marker shot noise has not been detected in experiments to date, even when sought: the effect has always been masked by electronic shot noise, discussed in the following section. It is interesting that, in principle at least, the study of marker shot noise affords a sound method for determining particle number concentration in sols.

Electronic shot noise

Because of its particulate nature every electric current exhibits a fluctuation noise, commonly called electronic shot noise. Suppose the number of electrons emitted by a phototube cathode in an interval Δt is n, whereas the number that would have been emitted in the absence of fluctuation noise is $\tilde{n}$. By the arguments of the preceding section $\overline{(n-\tilde{n})^2} = \bar{n}$.

Division of both sides by $(\Delta t)^2$ and multiplication by the electronic charge squared, e^2, transforms this to

$$\overline{(I_K-\bar{I}_K)^2} = e\bar{I}_K/\Delta t,$$

where I_K is the cathode current. Suppose Δt is defined by a low-pass filter of bandwidth Δf; we have $\Delta t = 1/2\Delta f$. Then

$$\overline{(I_K-\bar{I}_K)^2} = 2e\bar{I}_K\Delta f.$$

Except for the substitution of $\tilde{I}$ for $\bar{I}$ on the l.h.s., this is the well-known formula for electronic shot noise; see, for example, Parker (1950).

The multiplier stages of the phototube amplify the cathode shot noise, carrying through statistically unchanged the relative noise level

$$\frac{\overline{(I_K-\bar{I}_K)^2}}{\bar{I}_K^2} = \frac{2e\Delta f}{\bar{I}_K}.$$

However, more noise appears at each stage, in consequence of which the mean-square shot noise associated with the anode or ultimate output current I_A is (Philips Electron Tube Division 1964 *Philips Photomultiplier Tubes*. Holland)

$$\frac{\overline{i_A^2}}{\bar{I}_A^2} \simeq \frac{2e\Delta f}{\bar{I}_K}\frac{A_n}{A_n-1},$$

where A_n is the amplification factor per stage. Since A_n is usually about 5,

$$\frac{\overline{i_A^2}}{\bar{I}_A^2} \simeq \frac{2{\cdot}5e\Delta f}{\bar{I}_K} = \frac{2{\cdot}5Ae\Delta f}{\bar{I}_A}, \tag{9}$$

where A is the over-all gain. Thus about 80% of the noise originates at the photocathode, where the current is smallest.

Rearrangement of (9) shows that the spectral density function of the relative shot noise level approximates

$$\frac{\overline{i_A^2}|_{f,\Delta f}}{\bar{I}_A^2 \Delta f} \simeq \frac{2{\cdot}5e}{\bar{I}_K} = \frac{2{\cdot}5Ae}{\bar{I}_A}. \tag{10}$$

The relative shot noise level must be adequately low in the scattered-light technique. Equations (9) and (10) suggest the desirability of making the photocathode current large and of filtering the signal to reject noise from outside the turbulent frequency range when measuring the total intensity of concentration fluctuations and similar integral statistical quantities.

It is of interest that shot noise is random or 'white'; i.e. the spectral density is independent of frequency. Thus the noise generated by a steadily illuminated phototube has been useful in our work for calibrating filters and wave analysers. Through (9) it has also been used to determine the over-all phototube gain, A.

The total phototube response

All ordinarily significant components of the phototube response have now been considered. Collecting these gives for the mean anode current

$$\bar{I}_A = \bar{I}_s + \bar{I}_b + \bar{I}_d, \tag{11}$$

where $\bar{I}_s$ and $\bar{I}_b$ are the mean responses to light scattered from the object control volume and to background radiation, and $\bar{I}_d$ is the mean dark current. From (4) and (5),

$$\bar{I}_s = \tfrac{1}{4}\pi \overline{N} D_p^2 \omega_i \omega_s \int_0^\infty s \psi_{\mathrm{av}} \tau_1 \tau_2 \tau_L J_0 d\lambda. \tag{12}$$

The mean-square fluctuating current in a frequency interval from f to $f+\Delta f$ is

$$\overline{i_A^2}|_{f,\Delta f} = \{\overline{i_s^2} + \overline{i_0^2} + \overline{i_b^2} + \overline{i_{msn}^2} + \overline{i_{esn}^2}\}|_{f,\Delta f}, \tag{13}$$

where the terms on the r.h.s. represent the turbulent fluctuations in the continuum-wise marker content of the control volume, the ripple in the light source, the fluctuation in the background radiation (assumed statistically independent of $\overline{i_s^2}$), the marker shot noise, and the electronic shot noise. From the results in the preceding sections,

$$\overline{i_s^2}|_{f,\Delta f} = \frac{\overline{(\tilde{N} - \overline{N})^2}|_{f,\Delta f}}{\overline{N}^2} \bar{I}_s^2, \tag{14}$$

$$\overline{i_0^2}|_{f,\Delta f} = \overline{\beta^2}|_{f,\Delta f} \bar{I}_s^2, \tag{15}$$

$$\overline{i_{msn}^2}|_{f,\Delta f} \simeq \begin{cases} \dfrac{\pi D \Delta f}{2\overline{N}\,\overline{U}} \bar{I}_s^2 & (f + \Delta f < 2\overline{U}/\pi D), \\ 0 & (f > 2\overline{U}/\pi D), \\ \bar{I}_s^2/\overline{N} & (f = 0, \Delta f > 2\overline{U}/\pi D), \end{cases} \tag{16}$$

$$\overline{i_{esn}^2}|_{f,\Delta f} \simeq 2{\cdot}5Ae\bar{I}_A \Delta f. \tag{17}$$

To illustrate practical orders of magnitude, consider the signals developed through a low-pass filter with a bandwidth of 20,000 c/s, passing all turbulence frequencies in a case of interest. In a turbulent jet, the minimum magnitude of $\overline{(\tilde{N}-\bar{N})^2}/\bar{N}^2$ is on the order of 0·05. For a lamp with 1% r.m.s. ripple, $\beta^2 = 0{\cdot}0001$. The phototube anode current may be on the order of 10 μA and the over-all gain $A = 10^6$: the mean-square relative electronic shot noise level in $\Delta f =$ 20,000 c/s is then given by (17) (in which $e = 1{\cdot}6 \times 10^{-19}$ coulomb) as *ca.* 0·001 (assuming $\bar{I}_A \simeq \bar{I}_s$). If $\bar{U} = 30$ m/sec and $D = 1$ mm, then the marker shot noise is given by (7), in which $1/\bar{N} = 0{\cdot}001$ when $\bar{N} = 1000$. If $V \simeq D^3$, then $\bar{N} = 1000$ when $\bar{N}/V = 10^6$ particles/cm^3.

3. Marker adequacy

Colloidal particles used as markers must have small inertia and small tendency to evaporate, sublime, coagulate, or react chemically.

Small inertia is measured by the ability to follow the stream motion through sinusoidal velocity fluctuations of frequency f. The velocity amplitude ratio for a spherical particle acted on by the Stokes drag with the Cunningham correction is easily shown to be

$$u'/u = 1/[1+(2\mu f/a)^2]^{\frac{1}{2}},$$

where a is $18\mu/\rho_p D_p^2(1+Kl/D_p)$, u' and u are the r.m.s. velocities of the particle and the gas, l is the molecular mean free path of the gas, and K is the Cunningham constant (1·8 for air). Consider particles of density 1 g/cm^3 in air at ordinary temperature and pressure ($l = 10^{-5}$ cm, $\mu = 1{\cdot}9 \times 10^{-4}$ g/cm sec). The frequencies at which the velocity amplitude response is down 10% (i.e. $u'/u = 0{\cdot}9$) for particles of different sizes are:

D_p (mm $\times 10^3$)	0·1	0·3	1	3	10
f (c/s)	930,000	180,000	22,000	2700	250

In work to date, the turbulence energy has been concentrated in frequencies below 10,000 c/s, and the oil smokes used can be considered satisfactory if the particle size was below 2 microns. The Stokes diameter found by Rosensweig *et al.* (1961) was 0·5 microns.

The rate of evaporation of small droplets is set by molecular diffusion, and is proportional to the surface area. The theory of Langmuir (1918) gives

$$\frac{dD_p}{dt} = \frac{4M\mathscr{D}}{\rho_p D_p RT}(p-p_\infty), \tag{18}$$

where M and p are the molecular weight and vapour pressure of the droplet liquid, and $\mathscr{D}$ and p_∞ are the vapour diffusivity and partial pressure in the ambient gas. The vapour pressure p is affected by surface curvature:

$$p = p^\circ \exp\left[\frac{4\sigma M}{\rho_p D_p RT}\right],$$

where p° is the normal vapour pressure and σ is the surface tension of the liquid. For the oil used in our work (Nolan 1946) $\ln p^\circ = 25{\cdot}5 - 8220/T$, where p° is in

dynes/cm^2 and T in °K. For droplets larger than 0·1 micron diameter, the surface curvature is unimportant. The diffusivity of the vapour in air at 300 °K is 0·03 cm^2/sec, based on values quoted by Nolan (1946). Taking $M = 250$ g/mole, $\rho_p = 0{\cdot}9$ g/cm^3, and $D_p = 0{\cdot}4 \times 10^{-4}$ cm, Rosensweig *et al.* calculate the initial percentage rate of decrease of the particle diameter from (19) as 5% per sec. This is negligible in terms of the residence times (on the order of 0·01 to 1 sec) in systems studied to date.

Coagulation affects the particle size and number. For spherical liquid droplets the total mass m of particles inside the control volume V is $\pi\rho_p D_p^3 N/6$. This relation together with (3) and (4) indicates a signal strength I_s proportional to $m\psi_{\mathrm{av}}/D_p$. For small particles (Rayleigh scatter) ψ is proportional to D_p^4, and the signal is proportional to D_p^3. For large particles, on the other hand, $\psi \neq f(D_p)$ and the signal is inversely proportional to D_p.

In practice coagulation by Brownian collisions can be studied by putting sol in a cell and observing the change in the scattered-light signal with time. The coagulation of aerosols often follows a second-order rate expression (Whytlaw-Gray & Patterson 1932),

$$-\frac{dN}{dt} = k_r N^2/V. \tag{19}$$

The rate constant k_r for spherical particles which coagulate at contact is given by Smoluchowski's (1926) theory with the Cunningham correction as

$$k_r = \tfrac{4}{3}kT(1 + Kl/D_p)/\mu,$$

where k is Boltzmann's constant, T the absolute temperature,and μ the viscosity of the suspending medium. With these expressions for the coagulation rate, (3) and (4), and the relation $N = 6m/\pi\rho_p D_p^3$, it may be shown that for small particles (predominantly Rayleigh scatter)

$$\frac{dI_s}{dt} \propto 1 + \frac{Kl}{D_p},$$

while for large particles

$$-\frac{dI_s}{dt} \propto D_p^{-4}\left(1 + \frac{Kl}{D_p}\right).$$

Thus I_s increases with time at a diminishing rate for small particles, but decreases with time at a diminishing rate for large particles.

The variation of I_s with time facilitates a particle diameter classification according to whether I_s increases, decreases, or remains essentially constant. The regime of near constancy is around $\pi D_p/\lambda = \frac{1}{2}$. For our oil smokes I_s decreased very slowly with time: a 20% fall in 10 min was typical. Since residence times in fields of interest were under 1 sec, coagulation by Brownian collisions was clearly inconsequential. The central light wavelength, determined by the phototube, was *ca.* 0·5 micron. Since I_s decreased with time, it appears that the particles were larger than $\lambda/2\pi = 0{\cdot}1$ micron diameter. An upper limit on size is independently set as follows: from the absence of detectable marker shot noise, it appears that the number concentration of particles was greater than 10^5 particles/cm^3. For the maximum mass concentration of *ca.* 10^{-5} g/cm^3, the upper limit on particle diameter is thus calculated to be 5 micron. This range, 0·1–5 micron, brackets the experimental Stokes value of 0·5 micron.

It should be emphasized that the important coagulation effect is the variation in the signal I_s with time, and not the number concentration or size of the particles. In the above experiment the number concentration evidently decreased by Brownian collisions at about the same rate as I_s: for particles of 0·5 micron diameter, 0·9 g/cm^3 concentration, the percentage rate of decrease calculated from equation (19) is 0·4% per sec, or about 25% in 10 min.

Collisions between particles are produced also by small-scale turbulent motions of the fluid. According to Saffman & Turner (1956), from turbulent collisions alone

$$-\frac{dN}{dt} = 2\pi 2^{\frac{1}{2}} D_p^3 \frac{N^2}{V} \frac{\overline{(u^2)}^{\frac{1}{2}}}{\lambda_d},$$

where $\overline{(u^2)}^{\frac{1}{2}}$ is the r.m.s. velocity fluctuation in an isotropic turbulence and λ_d is the dissipation scale. For the jets investigated in our work,

$$\overline{(u^2)}^{\frac{1}{2}}/\lambda_d \cong 250 U_0 D_0/x^2$$

on the centre-line, where U_0 and D_0 are the nozzle velocity and diameter and x is distance from the nozzle. Under the worst conditions studied, $U_0 = 13{,}000$ cm/sec, $D_0 = 0{\cdot}6$ cm and $x = 10$ cm. With $D_p = 0{\cdot}5 \times 10^{-4}$ cm and $N/V = 10^6$ particles/cm^3, $d \ln N/dt = 0{\cdot}05\,\text{sec}^{-1}$. Since transit times from the nozzle to 40 cm downstream (the zone of interest) were on the order of 0·01 sec, this pessimistic calculation indicates that coagulation, even with the help of turbulence, was never significant.

4. Flow disturbance

As always, the system is disturbed by the act of observation. Particles in aerosols have been observed to move at speeds of several cm/sec in an intense light-beam (Whytlaw-Gray & Patterson 1932), but the effect is negligible in most systems of interest. The assumption that the fluid viscosity and density are effectively unaltered by the presence of the marker is undoubtedly justified for the oil smokes used in work to date, the maximum concentration of oil being generally below 0·01 weight fraction. The marker may also affect the fluid properties through processes of evaporation, adsorption, etc. Calculations of simultaneous heat and mass transfer show that the thermal effects of evaporation in our oil smokes are quite negligible.

5. Theory of the resolution of the point concentration

The response of the phototube to light scattered by particles inside the object control volume V can be written

$$\overline{I_s} = \frac{S}{V} \int \overline{\Gamma}^* dV \tag{20}$$

for the mean and

$$\overline{i_s^2} = \frac{S^2}{V^2} \overline{\left[\int_V \gamma^* dV \right]^2} \tag{21}$$

for the mean-square turbulent fluctuation, where

$$S \equiv \tfrac{1}{4}\pi D_p^2 V \omega_i \omega_s \int_0^\infty s\psi_{\mathrm{av}} \tau_1 \tau_2 \tau_L J_0 d\lambda$$

is the over-all system sensitivity,

$$\overline{\Gamma}^* \equiv \lim_{V \to 0} \frac{\overline{N}}{V},$$

and

$$\gamma^* \equiv \lim_{V \to 0} \frac{\hat{N} - \overline{N}}{V}.$$

The asterisk indicates identification with the marker particles; later we shall use Γ and γ without asterisks to denote the concentration of material of the marked stream. Since the object of measurements is normally to characterize the point values of concentrations, the conditions will now be considered under which (20) and (21) approach the desired limits

$$\bar{I}_s = S\overline{\Gamma}^* \quad \text{and} \quad \overline{i_s^2} = S^2\overline{\gamma^{*2}}.$$

Clearly the requirement is to make the control volume V small. Since, however, a decrease in V by itself increases the relative level of every kind of noise, a problem of optimization results.

The mean marker concentration

Suppose it is wished to measure the mean marker concentration Γ^* at a position $\mathbf{x}$. Let ξ be the distance along a line through $\mathbf{x}$ following the mean concentration gradient $\nabla\Gamma^*$. Expanding Γ^* about $\xi = 0$ at $\mathbf{x}$ in a Taylor series and neglecting terms higher than second order gives

$$\overline{\Gamma}^*(\xi) = \overline{\Gamma}^*(\mathbf{x}) + \xi\overline{\Gamma}^{*\prime}(\mathbf{x}) + \tfrac{1}{2}\xi^2\overline{\Gamma}^{*\prime\prime}(\mathbf{x}).$$

In work on jets, wakes, and diffusion plumes, the incident light-beam normally enters from the side of the flow and is directed parallel to $\nabla\Gamma^*$, in which case (20) can be written

$$\bar{I}_s = \frac{L}{S}\int_{-\frac{1}{2}L}^{\frac{1}{2}L} \Gamma^*(\xi) d\xi,$$

where L is the length of the cylindrical control volume. Also $\overline{\Gamma}^{*\prime\prime} = \nabla^2\overline{\Gamma}^*$. These expressions yield

$$\bar{I}_s = S[\overline{\Gamma}^*(\mathbf{x}) + \tfrac{1}{24}L^2\nabla^2\overline{\Gamma}^*(\mathbf{x})].$$

Thus $\bar{I}_s$ is a linear measure of $\overline{\Gamma}^*$ when $L^2\nabla^2\overline{\Gamma}^*(\mathbf{x}) \ll 24\overline{\Gamma}^*(\mathbf{x})$. This condition, which means that the concentration profile must not show large curvature within the control volume, is usually easy to satisfy.

Concentration fluctuation

The mean-square signal fluctuation in a frequency band from f to $f+\Delta f$ can be written, from (21),

$$\begin{aligned}\overline{i_s^2}|_{f,\Delta f} &= \frac{S^2}{V^2}\overline{\left[\int_V \gamma^* dV\right]^2}\Big|_{f,\Delta f} \\ &= \frac{S^2}{V^2}\int_V\int_V \overline{\gamma^{*\prime}\gamma^{*\prime\prime}}|_{f,\Delta f} dV'\,dV'' \\ &= \frac{S^2}{V^2}\int_V\int_V \overline{\gamma^{*\prime 2}}|_{f,\Delta f}\overline{\gamma^{*\prime\prime 2}}|_{f,\Delta f} C^*_{f,\Delta f}(\mathbf{x}',\mathbf{x}'')\,dV'\,dV'', \end{aligned} \tag{22}$$

where $\overline{\gamma^{*\prime}\gamma^{*\prime\prime}}|_{f,\Delta f}$ is the correlation between concentration fluctuations in volume elements dV' and dV'' located in V at positions $\mathbf{x}'$ and $\mathbf{x}''$, and $C^*_{f,\Delta f}(\mathbf{x}',\mathbf{x}'')$ is the correlation coefficient. If the object is to resolve $\overline{\gamma^{*2}}|_{f,\Delta f}$, the conditions for sufficient smallness of V are: (i) $\overline{\gamma^{*2}}|_{f,\Delta f}$ is essentially uniform over V, and (ii) $C^*_{f,\Delta f}(\mathbf{x}',\mathbf{x}'')$ is essentially unity for all pairs of points $\mathbf{x}'$ and $\mathbf{x}''$ within V. Of these conditions, the second is the more stringent. We therefore suppose the first to be adequately satisfied (usually not difficult) and obtain for the attenuation factor on $\overline{\gamma^{*2}}|_{f,\Delta f}$,

$$\begin{aligned} Q_{f,\Delta f} &\equiv \overline{\hat{\gamma}^{*2}}|_{f,\Delta f}/\overline{\gamma^{*2}}|_{f,\Delta f} \\ &\equiv \frac{1}{V^2}\int_0^L\int_0^L\int_0^{2\pi}\int_0^{2\pi}\int_0^R\int_0^R C^*_{f,\Delta f}(r',\phi',z';r'',\phi'',z'')\,dr'\,dr''\,d\phi'\,d\phi''\,dz'\,dz'', \end{aligned} \tag{23}$$

where

$$\hat{\gamma}^* \equiv \int_V \gamma^* dV,$$

and r, ϕ, z are cylindrical co-ordinates appropriate to the control volume of usual interest—of diameter $D \equiv 2R$ and length L.

Equation (23) can be solved analytically in one limiting case. Suppose the correlation coefficient depends only on the separation distance ζ,

$$\zeta \equiv [(r'\cos\phi' - r''\cos\phi'')^2 + (r'\sin\phi' - r''\sin\phi'')^2 + (z'-z'')^2]^{\frac{1}{2}}.$$

A series expansion about $\zeta = 0$ gives the parabolic approximation

$$C^*_{f,\Delta f}(\zeta) = 1 - \alpha\zeta^2. \tag{24}$$

Equation (23) then yields

$$Q_{f,\Delta f} = 1 - \tfrac{1}{6}\alpha(L^2 + \tfrac{3}{2}D^2). \tag{25}$$

For our control volumes, $L = 0{\cdot}8D$ and

$$Q_{f,\Delta f} = 1 - 0{\cdot}323\alpha D_V^2, \tag{26}$$

where D_V is the diameter of a sphere of volume $V = \pi D^2 L/4$. An L/D value of unity gives 0·318 for the numerical coefficient so the result in this form is insensitive to mild variations in control volume shape.

Numerical solutions of (23) for several forms of the correlation coefficient have been obtained on a digital computer and are presented together with experimental data in § 6.

The spectral density function

In the limit $\Delta f \to 0$, equation (23) gives the volume attenuation factor on the frequency spectral density function, $G^*(f)$,

$$G^*(f) \equiv \lim_{\Delta f \to 0} \frac{\overline{\gamma^{*2}}|_{f,\Delta f}}{\Delta f}.$$

The correlation coefficient is then that, C_f^*, between concentration fluctuations of a single frequency.

To a fair approximation, the concentration fluctuations in V can usually be regarded as due to the convection of a frozen concentration field through V at the mean stream velocity $\overline{U}$. Then

$$G^*(f) \simeq \frac{2\pi}{\overline{U}} E^*(\kappa),$$

where $E^*(\kappa)$ is the one-dimensional wave-number spectral density function and $\kappa \simeq 2\pi f/\overline{U}$ is the wave-number component in the direction of mean motion. Equation (23), written for $E^*(\kappa)$, then involves the correlation coefficient C_κ^* between marker concentration fluctuations of wave-number κ. For pairs of points separated only in the mean flow direction we should have (a single Fourier component)

$$C_\kappa^* = \cos \kappa\zeta. \tag{27}$$

For other points the field structure over all values of the transverse wave-number components affects the result.† However, (27) should still afford a rough approximation to the limit case of small separation distances, $\zeta \to 0$. The resulting value of α in the parabolic approximation equation (24) is $\frac{1}{2}\kappa^2$. The attenuation factor on $E^*(\kappa)$ for our control volumes is then, from (26),

$$Q_\kappa = 1 - 0{\cdot}16\kappa^2 D_V^2. \tag{28}$$

The total mean-square concentration fluctuation

The total mean-square marker concentration fluctuation in all frequencies or wave-numbers is

$$\overline{\gamma^{*2}} \equiv \lim_{\Delta f \to \infty} \overline{\gamma^{*2}}|_{0,\Delta f} = \int_0^\infty G^*(f)\,df$$

$$= \int_0^\infty E^*(\kappa)\,d\kappa. \tag{29}$$

However, in the light-scatter technique volume-averaging produces rapid attenuation of the spectral response at large wave-numbers. Thus the measurement of $\overline{\gamma^{*2}}$, as suggested by (28), is effectively truncated at a wave-number on the order of $\kappa_V = 1/D_V$. Since there are practical limits on the diminution of the con-

† In a more general argument the wave-number component in the mean-flow direction, here denoted by κ unadorned, would be written κ_1, and the transverse components, κ_2 and κ_3.

trol volume size, set by the increase in relative noise level, etc., a question arises as to the significance of the measurable quantity

$$\overline{\gamma^{*2}}|_{0,\kappa_V} = \int_0^{\kappa_V} E^*(\kappa)\,d\kappa.$$

To answer this it is necessary to consider the form of the spectrum over all wave-numbers.

It is an important characteristic of marker sols that the particle diffusivity $\mathscr{D}^*$ in the suspending medium is much smaller than the kinematic viscosity of the medium, ν. Thus the effective Schmidt number of the particles is enormous, $\nu/\mathscr{D}^* > > > 1$. The equilibrium spectrum of turbulent concentration fluctuations under this condition has been examined by Batchelor (1959): the low wave-number end develops into a Kolmogoroff subrange in which the spectral density is proportional to $\kappa^{-\frac{5}{3}}$. Then, at a wave-number on the order of $(\epsilon/\nu^3)^{\frac{1}{4}}$ (where ϵ is the turbulence energy dissipation rate), beyond which the velocity eddies are rapidly dissipated by viscosity, the continuing insignificance of particle diffusion comes into evidence and transition takes place to a second convection subrange in which the spectral density varies as κ^{-1}. Finally, at a wave-number on the order of $(\epsilon/\nu\mathscr{D}^{*2})^{\frac{1}{4}}$ the marker concentration eddies do begin to dissipate by particle diffusion, and from there on the spectral density falls rapidly. Thus, if it is desired to evaluate the total mean-square marker concentration $\overline{\gamma^{*2}}$ as given by (29), the control volume cut-off wave-number κ_V must be in the neighbourhood of, or larger than, the particle diffusion cut-off value for the (-1)-power subrange:

$$\overline{\gamma^{*2}} = \int_0^{\infty} E^*(\kappa)\,d\kappa = \int_0^{\kappa_V} E^*(\kappa)\,d\kappa \quad \text{if} \quad \kappa_V \geqslant (\epsilon/\nu\mathscr{D}^*)^{\frac{1}{4}}.$$

It seems that $\overline{\gamma^{*2}}$ would become infinite if the (-1)-power region extended upward without bound. Actually, as noted by Rosensweig (1959), a limit on $\overline{\gamma^{*2}}$ is independently set by the fact that at any point in a turbulent field the straining of the marker continuum filaments and sheets can only have proceeded a finite way. If the initial uniform marker concentration in the marked stream is Γ_0^*, then in the absence of marker diffusion the concentration of the marker in portions of fluid containing it remains steadily Γ_0^*. It is easily shown that then

$$\overline{\gamma^{*2}} = \omega(1-\omega)\Gamma_0^{*2}$$

and

$$\overline{\gamma^{*2}}/\overline{\Gamma}^{*2} = (1-\omega)/\omega,$$

where ω is the volume fraction of marked fluid in the local mixture.

In systems studied to date the upper wave-number limit of the (-1)-power region of the spectrum has been utterly beyond reach, and it appears that no refinements are feasible which will allow the use of a small enough control volume to bring the very high wave-number region into focus and yet not lose the signal in noise. Indeed it has not yet been possible to detect even the beginning of the (-1)-power convection subrange. The prospects are hopeful, however, and a future effort directed toward this goal may succeed.

Concentration fluctuations in the marked material

The marker is normally chosen to follow as faithfully as possible the turbulent motions of the mixing fluids. To this extent it identifies the material of the marked stream. In isopycnic mixing $\Gamma^*/\Gamma_0^* = \Gamma/\Gamma_0$,

where Γ is the concentration of marked material and Γ_0^* and Γ_0 are the initial uniform concentrations of marker and marked material in the marked stream at entry to the mixing field.

Since the diffusivities of the marker particles and the molecules of the marked material differ widely, the ability of the marker to represent the concentration fluctuations of the marked material is limited to the wave-number range $\kappa < \kappa_c$ in which the fluctuations of both are in the convection ranges of their spectra. The limiting wave-number is determined by whichever species has the lower limit on its convection range, and is on the order of (based on the discussions of scalar-fluctuation spectra by Batchelor (1959) and Batchelor, Howells & Townsend (1959))

$$\kappa_c = (\epsilon/\mathscr{D}^3)^{\frac{1}{4}} \quad \text{if } \mathscr{D} > \nu \quad \text{and} \quad \mathscr{D} > \mathscr{D}^*,$$

$$\kappa_c = (\epsilon/\nu\mathscr{D}^2)^{\frac{1}{4}} \quad \text{if } \mathscr{D} < \nu \quad \text{and} \quad \mathscr{D} > \mathscr{D}^*,$$

and (an artificial case)

$$\kappa_c = (\epsilon/\nu\mathscr{D}^{*2})^{\frac{1}{4}} \quad \text{if} \quad \mathscr{D} < \nu \quad \text{and} \quad \mathscr{D} < \mathscr{D}^*,$$

where $\mathscr{D}^*$ and $\mathscr{D}$ are the diffusivities of the marker and the marked species.

If, as is normally true, $\mathscr{D} > \mathscr{D}^*$, then the total mean-square fluctuation in the concentration of marked material in isopycnic mixing should be represented within 1% error by

$$\overline{\gamma^2} = \int_0^\infty E(\kappa)\,d\kappa \simeq \frac{\Gamma_0^2}{\Gamma_0^{*2}} \int_0^{\kappa_c} E^*(\kappa)\,d\kappa.$$

To measure $\overline{\gamma^2}$ by the scattered-light technique it is thus only necessary to put the marker fluctuation signal through a filter with a passband from 0 to κ_c. This filtration can be provided either by an appropriate choice of control volume size or by a low-pass electronic filter operating on the phototube output.

The effect of control volume size on the measurement of $\overline{\gamma^2}$ can be calculated from the effect on the spectrum:

$$\frac{\overline{\hat{\gamma}^2}}{\overline{\gamma^2}} \simeq \left.\frac{\overline{\hat{\gamma}^{*2}}}{\overline{\gamma^{*2}}}\right|_{0,\kappa_c} = \frac{\int_0^{\kappa_c} Q_\kappa E^*(\kappa)\,d\kappa}{\int_0^{\kappa_c} E^*(\kappa)\,d\kappa}, \tag{30}$$

where

$$\hat{\gamma} \equiv \frac{1}{V}\int_V \gamma\,dV.$$

It can also be calculated from (23) by setting $f = 0$ and $\Delta f = \overline{U}\kappa_c/2\pi$. The correlation coefficient in (23) becomes that between concentration fluctuations in the

marked material, namely $C(\mathbf{x}', \mathbf{x}'') = \overline{\gamma'\gamma''}/\overline{\gamma^2}$. At the relatively small separation distances $\zeta \equiv |\mathbf{x}' - \mathbf{x}''|$ normally occurring within a properly sized control volume, C can be expected to depend primarily on ζ. At very small ζ, the parabolic approximation, (24), might seem appropriate. However, the parabolic behaviour reflects the effects of molecular diffusion and these are masked in the light-scatter technique. The parabolic region is in any case usually very small. Thus a more realistic approximation is usually one of the forms

$$C(\zeta) = 1 - a\zeta/\Lambda, \tag{31}$$

$$C(\zeta) = \exp\{-b\zeta/\Lambda\}, \tag{32}$$

where Λ is the longitudinal integral scale, discussed in §7, and a and b are constants. These forms should be reasonably accurate up to $\zeta = \frac{1}{2}\Lambda$, and should give good results if the control volume dimensions D and L are smaller than $\frac{1}{2}\Lambda$.

Solutions for the attenuation factor on $\overline{\gamma^2}$ from (23), (31) and (32) by the foregoing argument have been obtained on a digital computer and are presented together with experimental results in §6.

6. Experimental studies on the resolution of concentration fluctuations

Experiments were carried out to demonstrate the theoretical relations obtained in the preceding sections and establish completely quantitative correction procedures for the treatment of data.

The light-scatter system

An air–oil condensation smoke was used as a marker. The light source was a 100 W zirconium arc lamp provided with five round apertures to control the beam diameter D in the object segment. Slitted diaphragms with three slit sizes placed before the phototube controlled the segment length L.

The control volumes were geometrically similar to an adequate degree, with $L/D \simeq 0{\cdot}8$, and are characterized as to scale by the equivalent spherical diameter $D_V = (6V/\pi)^{\frac{1}{3}}$, where $V = \frac{1}{4}\pi D^2 L$. The incident beam divergence angle ω_i was below 0·01 steradian and the scattered beam divergence ω_s was about 0·2 steradian. The phototubes were selected for high cathode photosensitivity in order to minimize the relative electronic shot noise and dark noise levels (selection is important, for the variability is great).

Spectra in a free jet

The marker concentration fluctuation spectrum in a round free jet of smoke-marked air mixing with clear room air at uniform temperature was studied at a point on the jet centre-line 64 nozzle radii from the nozzle at a nozzle Reynolds number $D_0 U_0/\nu$ of 54,000. The nozzle was a 0·635 cm throat diameter flow nozzle giving a uniform effluent velocity distribution.

Spectra were measured with a sound analyser the passband of which is a constant fraction of the tuned frequency, nominally $0{\cdot}04f$ or $0{\cdot}12f$. The $0{\cdot}12f$ bandwidth was used only in the initial white portion of the spectrum. The analyser

was calibrated against white noise. The analyser output was measured with a random signal voltmeter accurate to $\pm\frac{1}{2}\%$.

Figure 2 shows the measured spectra. The attenuation of the frequency response with increasing control volume diameter is very evident. At the high-frequency end the spectral density levels off at the electronic shot noise level

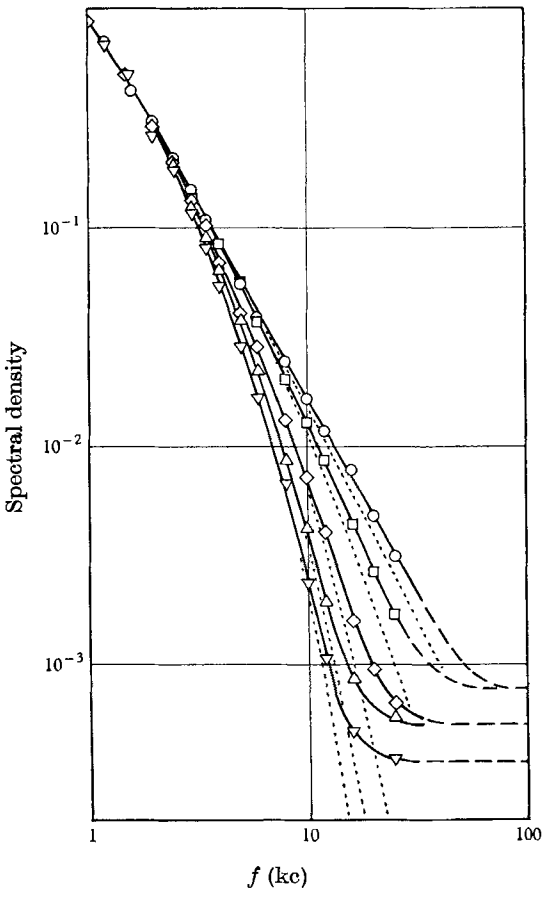

FIGURE 2. Spectra on the jet centre-line 64 nozzle radii from the nozzle mouth. Nozzle air velocity, 122 m/sec; local mean velocity, 30·5 m/sec. Control volume diameter $D_V = (6V/\pi)^{\frac{1}{3}}$ mm: ○, 0·85; □, 1·01; ◇, 1·64; △, 2·02; ▽, 2·25. At high frequencies the spectra level off at the random noise level, which was independently determined. The dashed curves represent the spectra with the random noise subtracted.

associated with the mean phototube current. The noise spectral density is essentially frequency-independent (white), and is therefore easily subtracted from the total response. However, the remainder quickly becomes smaller than the subtrahend and is lost in the experimental error. Thus the ultimate limit on the discrimination of marker concentration fluctuations in these experiments was not spatial resolution, but noise.

The simplest theoretical expectation for the attenuation factor Q_κ on the spectral density function is that it should depend on κD_V. Thus, proceeding empirically, a semilogarithmic relation between the measured spectral density and D_V^2 was found to be essentially linear at all frequencies (figure 3). The slopes

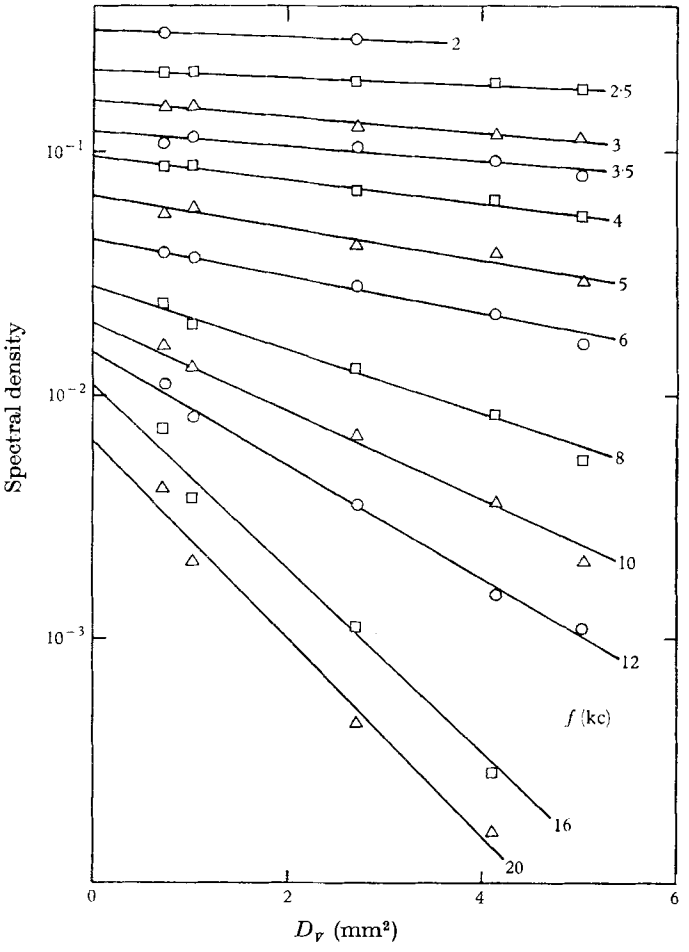

FIGURE 3. The spectral density function (corrected for random noise) as a function of the control volume diameter at different frequencies.

of the straight lines were then plotted on a log–log graph against κ^2 (figure 4), and found to be fairly well described by the dimensionally homogeneous relation (slope) $= -0{\cdot}12\kappa^2$. The resulting equation for the spectral attenuation is

$$Q_\kappa = \exp\{-0{\cdot}12\kappa^2 D_V^2\}. \tag{33}$$

At small values of κD_V this approaches

$$Q_\kappa = 1 - 0{\cdot}12\kappa^2 D_V^2, \tag{34}$$

in close agreement with the theoretical approximation for very small κD_V (equation (28)).

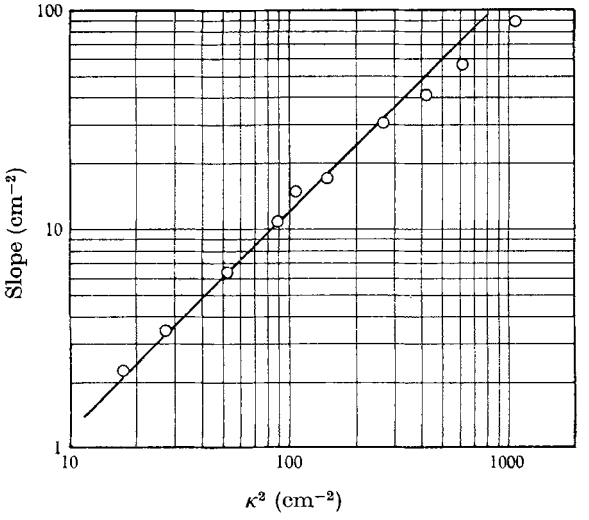

FIGURE 4. The slopes of the straight lines in figure 3 as a function of the wave-number squared.

It may now be asked what directionally averaged representation of the correlation coefficient as a function of separation distance alone leads from the theoretical response (equation (23)), to the experimental result (equation (33)). We have determined that a close approximation is

$$C_\kappa(\zeta) = \frac{\sin 1{\cdot}5\kappa\zeta}{1{\cdot}5\kappa\zeta}, \tag{35}$$

as shown by the following comparison:

κD_V	0·616	1·233	2·46	3·70	4·92
Q_κ, experiment	0·955	0·834	0·483	0·193	0·054
Q_κ, theory	0·955	0·834	0·470	0·161	0·023

Figure 5 shows the spectrum for the smallest control volume, corrected for both shot noise and volume attenuation. The first convection subrange, characterized by the $(-\frac{5}{3})$-power law, is very evident. The high wave-number limit of this subrange, *ca.* $\kappa = (\epsilon/\nu^3)^{\frac{1}{4}}$, is estimated as follows. In isotropic turbulence the energy dissipation rate is on the order of $\epsilon = 15\nu\overline{u^2}/\lambda_d^2$, where $\overline{u^2}$ is the mean-square velocity fluctuation and λ_d the dissipation scale. Along the centre-line of a turbulent jet and far from the nozzle, $\overline{u^2} \simeq (2D_0U_0/x)^2$ and $\lambda_d \simeq 0{\cdot}006x$, where D_0 is the nozzle diameter, U_0 the velocity at the nozzle, and x the distance from the nozzle. In the present case $x = 20$ cm and $D_0U_0/\nu = 54{,}000$, giving $\kappa = 400\ \text{cm}^{-1}$ for the transition wave-number. The experimental data extended only to $\kappa = 50\ \text{cm}^{-1}$ and the capability of the system could not be significantly extended. None the less, with an improved system, a larger jet, and all factors optimized, the limit of the $(-\frac{5}{3})$-power regime and the beginning of the (-1)-power regime beyond should be accessible.

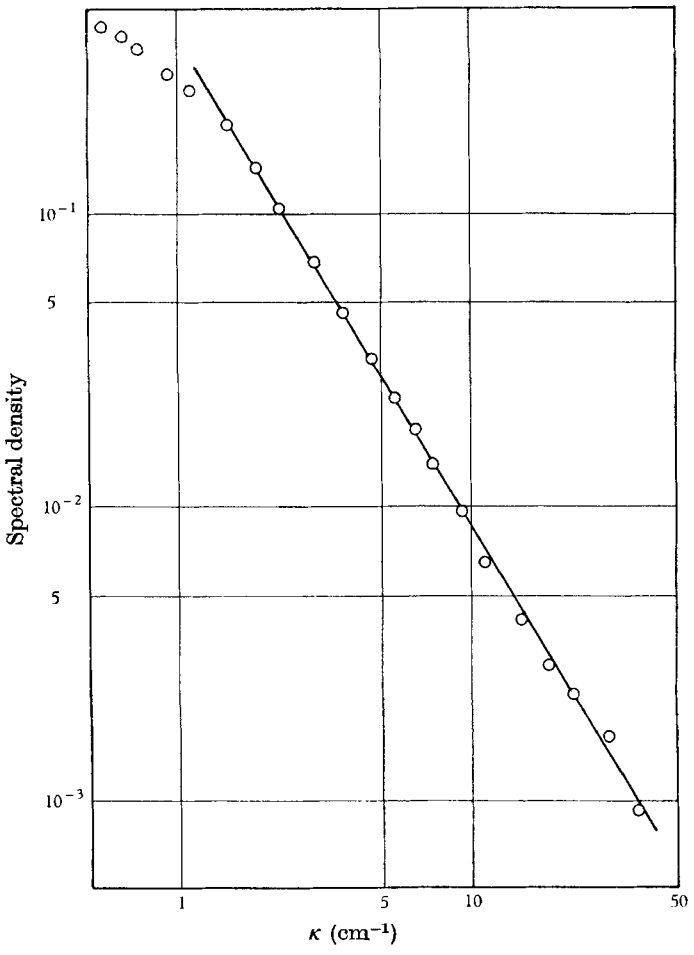

FIGURE 5. The spectrum corrected for the effects of random noise and control volume size. The straight line represents a $(-\frac{5}{3})$-power relation.

The upper limit of the (-1)-power subrange for the oil-smoke marker will be calculated for interest. The diffusivity of the smoke particles is estimated from the Stokes–Einstein formula with Cunningham correction,

$$\mathscr{D}^* = \frac{kT}{3\pi\mu D_p}[1 + Kl/D_p].$$

For particles of $0{\cdot}5 \times 10^{-4}$ cm diameter and air at room temperature, $\mathscr{D}^* = 4 \times 10^{-6}$ cm^2/sec, a value comparable to diffusivities in liquids. The Schmidt number of the particles in air is $\nu/\mathscr{D}^* = 0{\cdot}15/(4 \times 10^{-6}) = 3{\cdot}8 \times 10^4$. The cut-off wave-number for the (-1)-power subrange is about

$$\kappa = (\epsilon/\nu\mathscr{D}^{*2})^{\frac{1}{4}} = (\nu/\mathscr{D}^*)^{\frac{1}{2}}(\epsilon/\nu^3)^{\frac{1}{4}}.$$

Putting $(\epsilon/\nu^3)^{\frac{1}{4}} = 400$ and $\nu/\mathscr{D}^* = 3{\cdot}8 \times 10^4$, we find $\kappa = 80{,}000$. In the present experimental system, a control volume small enough to resolve concentration fluctuations at this level would contain an average of about 0·1 smoke particles.

Since the measured marker spectra were confined to the convection range of air mixing with air at constant temperature (molecular diffusion cut-off with $\mathscr{D} \simeq \nu$), the data are completely interpretable as the concentration fluctuation spectrum of the nozzle air in the jet:

$$E^*(\kappa)/\Gamma_0^{*2} \simeq E(\kappa)/\Gamma_0^2,$$

where $E(\kappa)/\Gamma_0^2$ is in fact the spectral density of fluctuations in the volume fraction of nozzle air.

Equation (33) is generally recommended as a basis for correcting measured spectra for the effects of control volume size. Normally these effects will become pronounced in the $(-\frac{5}{3})$-power or equivalent wave-number region, just as in the present work, and hence similar results should be expected.

The total mean-square concentration fluctuation of nozzle fluid in a free jet

In §5 we showed how the scattered-light technique can be used to measure the total mean-square fluctuation, $\overline{\gamma^2}$, in the concentration of material of the marked stream. The effects of control volume size on the measurement of $\overline{\gamma^2}$ can be calculated from the jet spectra described in §6 rather easily, because the attenuation of the spectral density function was effectively confined to wave-numbers beginning in the $(-\frac{5}{3})$-power convection equilibrium subregime. The complete data, to be presented elsewhere, give for this subrange

$$E(\kappa) = 0{\cdot}40\overline{\gamma^2}\Lambda^{-\frac{2}{3}}\kappa^{-\frac{5}{3}},$$

where Λ is the longitudinal integral scale of the fluctuations in the concentration of nozzle air, in value 0·90 cm. On substituting this relation for the spectral density function and (33) for the spectral attenuation factor, equation (30) yields

$$\left.\begin{aligned}\frac{\overline{\hat{\gamma}^2}}{\overline{\gamma^2}} &\simeq 1 - 0{\cdot}4\Lambda^{-\frac{2}{3}}\int_0^{\kappa_c}(1-\exp\{-0{\cdot}12\kappa^2 D_V^2\})\,\kappa^{-\frac{2}{3}}d\kappa \\ &\simeq 1 - 0{\cdot}4(D_V/\Lambda)^{\frac{2}{3}}\int_0^{\infty}(1-\exp\{-0{\cdot}12y^2\})\,y^{-\frac{5}{3}}dy \\ &\simeq 1 - 0{\cdot}4(D_V/\Lambda)^{\frac{2}{3}}\end{aligned}\right\} \tag{36}$$

(the extension of the integration range from κ_c to infinity gives little error).

Experiments were also carried out in which the effect of control volume size on $\overline{\gamma^2}$ was measured directly at points on the jet axis 16, 24 and 32 nozzle radii from the nozzle mouth: shot noise from wave-numbers above κ_c was removed by a 40,000 c/s low-pass filter, and the remainder was subtracted after calibrating it as a function of the mean phototube current. Now, when the integral effect of control volume size is small, as in the present work, the significant spectral contributions are concentrated in the higher wave-number regions, and, if in these the $(-\frac{5}{3})$-power law is obeyed, the integral attenuation factor is given by the generalization of (36),

$$\overline{\hat{\gamma}^2}/\overline{\gamma^2} = 1 - K(D_V/\Lambda)^{\frac{2}{3}}, \tag{37}$$

where the substitution of K for 0·4 as the numerical constant allows for variation in the shape of the spectrum. Figure 6*a* therefore shows a graph of the data after

equation (37). A linear relation is indeed approximated with different values of the constant K: at 16 nozzle radii downstream, $K = 0{\cdot}41$; at 24 radii, 0·27; and, at 32 radii, 0·33. The first and last values are close to that in equation (37), 0·4, from the spectrum at 64 nozzle radii.

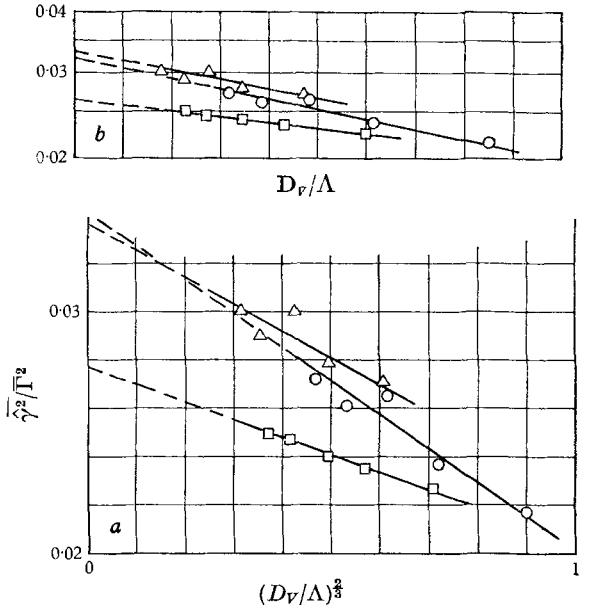

FIGURE 6. The effect of control volume size on the measured mean-square concentration fluctuation (*a*) after equation (37), bottom graph, and (*b*) after equation (40), top graph.

While a Kolmogoroff equilibrium subrange is not universal, it is quite common for the spectral density function to exhibit a power law behaviour in the same general range of wave-numbers:

$$E(\kappa) \propto \overline{\gamma^2}\Lambda^{-(n-1)}\kappa^{-n},$$

where n may be as high as 2. With this law for the spectral density and equation (33) for the attenuation factor, the solution of (30) for $n = 2$ is

$$\overline{\hat{\gamma}^2}/\overline{\gamma^2} = 1 - KD_V/\Lambda, \tag{38}$$

where K is an experimental constant.

The integral attenuation factor is also predictable from (23). Numerical solutions have been computed for control volumes with aspect ratios L/D of 0·7, 1·0 and 1·5. With equation (31) for the correlation coefficient, the result for aspect ratios of 0·7 and 1·0 is

$$\overline{\hat{\gamma}^2}/\overline{\gamma^2} = 1 - 0{\cdot}525aD_V/\Lambda, \tag{39}$$

while with equation (32)

$$\overline{\hat{\gamma}^2}/\overline{\gamma^2} = \exp\{-0{\cdot}525bD_V/\Lambda\}, \quad \overline{\hat{\gamma}^2} > \overline{\gamma^2}/2. \tag{40}$$

The results for $L/D = 1{\cdot}5$ are analogous in form but with a numerical coefficient of 0·550. Figure 6*b* shows a graph of the experimental data after equation (40).

The values of the coefficient b at 16 and 32 nozzle radii downstream position, 0·94 and 0·85, are in good accord with direct measurements of correlation coefficients in jets, representing a reasonable mean of the longitudinal and transverse values (see, for example, our 1967 paper). The use of (39) gives slightly less satisfactory results.

As a general basis for the correction of data on the total mean-square concentration fluctuation when the exact form of the spectrum is unknown, (40) appears to be the best compromise solution.

7. Other measurements

We have shown how the scattered-light technique is used to measure the mean, the total mean-square fluctuation, and the fluctuation spectrum of the concentration of material of the marked stream. The measurement of some other statistical parameters is now briefly described.

Correlation coefficients

If the incident light projection angle ω_i is made small and the system is set up to view with two phototubes through two slits two distinct segments of the incident beam, then the correlation can be measured between the volume-average concentration fluctuations in two equal volumes V' and V'' a distance ζ apart. When V' and V'' are sufficiently small the correlation $\overline{\gamma'\gamma''}$ is closely approximated. The criteria for sufficient smallness of control volume size may be appreciated from the effect on the spectrum. We have in this way made an extensive study of lateral correlation coefficients in jets. An analogue system (a correlation amplifier and random signal voltmeter) allowed the correlation coefficient

$$C \equiv \overline{\gamma'\gamma''}/(\overline{\gamma'^2}\overline{\gamma''^2})^{\frac{1}{2}}$$

to be read directly on a special scale.

A systematic study of the effects of control volume size on the two-point correlation coefficient, coupled with a rigorous theoretical analysis, has not yet been carried out. However, an effect has been detected empirically and the empirical correction may accordingly be applied until a better procedure is available. Consider the data on the symmetrical lateral coefficient in the free jet (figure 7, top three curves). Over most of the range the coefficient is a linear function of the centre-to-centre separation distance. Extrapolation of the straight lines to the ordinate $C = 1$ gives a constant intercept on the abscissa, $\zeta_1 = 1{\cdot}5\,\text{mm}$, independent of axial position in the jet. The true correlation should, however, be a simple curve extrapolating to $\zeta = 0$ at $C = 1$. The most obvious explanation of the difference is that the *effective* separation distance is not the measured centre-to-centre distance, but that distance minus a displacement error ζ_1. If so, the magnitude of ζ_1 should be consistent with the control volume length L; this was, significantly, 1·5 mm. Figure 7, bottom curve, shows the same data corrected and normalized. Complete data, including large separation distances, are given in our 1967 paper.

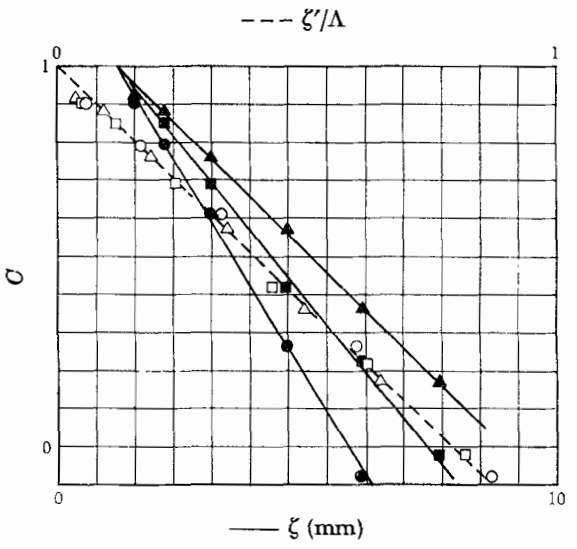

FIGURE 7. The symmetrical lateral correlation coefficient as a function of the separation distance in a free jet. Solid curves, the raw data; dashed curve, the data corrected for the displacement error and normalized with respect to the axial integral scale of the concentration fluctuations. The axial positions x/r_0 are: O●, 40; □■, 56; △▲, 72.

Longitudinal integral scale

The longitudinal correlation coefficient is obtained from the spectrum through the well-known Fourier transform relation

$$C(\zeta) = \frac{1}{\overline{\gamma^2}} \int_0^\infty E(\kappa) \cos(\kappa\zeta) d\kappa.$$

The longitudinal integral scale is

$$\Lambda \equiv \int_0^\infty C(\zeta) d\zeta.$$

The inverse Fourier transform is

$$E(\kappa) = \frac{2}{\pi} \overline{\gamma^2} \int_0^\infty C(\zeta) \cos(\kappa\zeta) d\zeta,$$

from which

$$\Lambda = \frac{\pi}{2} \frac{E(0)}{\overline{\gamma^2}} \equiv \frac{1}{4} \frac{\overline{U}}{\overline{\gamma^2}} \lim_{f \to 0} \frac{\overline{\gamma^2}|_{f, \Delta f}}{\Delta f}.$$

The last relation indicates a simple method for determining $E(0)$ and Λ. At low enough wave-numbers, the one-dimensional spectrum is usually 'white', i.e.

$$E(\kappa) = E(0) = \frac{\overline{U}}{2\pi} \frac{\overline{\gamma^2}|_{0, \Delta f}}{\Delta f}.$$

If $\overline{\gamma^2}|_{0, \Delta f}$ is measured within the white region by putting the phototube signal through a low-pass filter of white-noise bandwidth Δf, and $\overline{\gamma^2}$ is measured by putting the signal through a low-pass filter of bandwidth $\Delta f = \overline{U}\kappa_c/2\pi$, then we get Λ directly from these two measurements. This is the most accurate method

for determining both Λ and $E(0)$ and we have used it extensively in our work on jets. If $\overline{\gamma^2}|_{0,\Delta f}$ is no more than 5 to 10 % of $\overline{\gamma^2}$, it is normally safe to assume that Δf is in the white part of the spectrum.

Intermittency factor

The intermittency factor is defined as the probability, prob ($\Gamma > 0$), that the instantaneous concentration of material of the marked stream is greater than zero at a point. A system for measuring this factor has been developed and data on turbulent jets have been reported (Becker *et al.* 1965).

Large control volumes

From the discussion of the effects of control volume size it is evident that these can be turned to advantage: large control volumes giving e.g. a line or sheet sampling of space, can be utilized to study the properties of the spectrum and correlation functions. Sheet illumination has already been used to study the statistical properties of cross-sections of a diffusion plume (Becker *et al.* 1966).

8. Conclusion

It is evident that the scattered-light technique as so far developed is essentially a tool for investigating the convection ranges of the concentration fluctuation spectrum. It cannot give information about the mixing of gases in the spectral region where molecular diffusion is important, because marker sol particles do not portray gas behaviour at this level. However, the Schmidt numbers of sol particles in gases are similar to those of liquid pairs in important cases of liquid mixing, and hence the marker sol behaviour in *gas mixing* may portray reasonably well certain cases of liquid mixing.

This work was supported by the U.S. Army Research Office (Durham) under Grant no. DA-ARO(D)D-31-124-61-G55, Project no. 2013-E.

REFERENCES

Batchelor, G. K. 1959 *J. Fluid Mech.* **5**, 113.

Batchelor, G. K., Howells, I. D. & Townsend, A. A. 1959 *J. Fluid Mech.* **5**, 134.

Becker, H. A., Hottel, H. C. & Williams, G. C. 1963 Mixing and flow in ducted turbulent jets. *Ninth Symposium (International) on Combustion*, p. 7.

Becker, H. A., Hottel, H. C. & Williams, G. C. 1965 Concentration intermittency in jets. *Tenth Symposium (International) on Combustion*, p. 1253.

Becker, H. A., Hottel, H. C. & Williams, G. C. 1967 Concentration fluctuations in ducted turbulent jets. *Eleventh Symposium (International) on Combustion*, p. 791.

Becker, H. A., Rosensweig, R. E. & Gwozdz, J. R. 1966 Turbulent dispersion in a pipe flow. *A.I.Ch.E. J.* **12**, 964.

Bendat, J. S. 1958 *Principles and Applications of Random Noise Theory*. New York: Wiley.

Erickson, W. D. 1961 Light scattering: a technique for studying soot in flames. Sc.D. Thesis, Department of Chemical Engineering, Massachusetts Institute of Technology, Cambridge, Massachusetts.

GUCKER, F. T. & COHN, S. H. 1953 *J. Colloid Sci.* **8**, 550.

GURNITZ, R. N. 1966 Development and application of a light scattering technique for the study of premixed turbulent flames. Sc.D. thesis, Department of Chemical Engineering, Massachusetts Institute of Technology, Cambridge, Massachusetts.

HOTTEL, H. C., WILLIAMS, G. C. & MILES, G. A. 1967 Mixedness in the well-stirred reactor. *Eleventh Symposium (International) on Combustion*, p. 771.

LANGMUIR, I. 1918 *Phys. Rev.* **12**, 368.

NOLAN, J. T. 1946 Particle size of smoke from induction nozzles. Sc.D. thesis, Department of Chemical Engineering, Massachusetts Institute of Technology, Cambridge, Massachusetts.

PARKER, P. 1950 *Electronics*. London: Edward Arnold.

ROSENWEIG, R. E. 1959 Measurement and characterization of turbulent mixing. Sc.D. thesis, Department of Chemical Engineering, Massachusetts Institute of Technology, Cambridge, Massachusetts.

ROSENSWEIG, R. E., HOTTEL, H. C. & WILLIAMS, G. C. 1961 Smoke-scattered light measurement of turbulent concentration fluctuations. *Chem. Eng. Sci.* **15**, 111.

SAFFMAN, P. G. & TURNER, J. S. 1956 *J. Fluid Mech.* **1**, 16.

SMOLUCHOWSKI, Z. 1926 *Kolloid-Chem. Beih.* **22**, 126.

VAN DE HULST, H. C. 1957 *Light Scattering by Small Particles*. New York: Wiley.

WHYTLAW-GRAY, R. & PATTERSON, H. S. 1932 *Smoke*. London: Edward Arnold.

WILLIAMS, G. C. & BECKER, H. A. 1963 *Tappi*, **46**, 153A.